RESEARCH PROGRESS IN MECHANICAL AND MANUFACTURING ENGINEERING
e-ISSN: 2773-4765

RPMME

Vol. 7 No. 1 (2026) 114-126
https://publisher.uthm.edu.my/periodicals/index.php/rpmme

Characteristics and the Effect of Feldspar Reinforcement on Compression Strength Towards Various Types of Clay

Mohamad Zulfadhli Mohamad Nizam[1], Noradila Abdul Latif[1*]

[1] *Faculty of Mechanical and Manufacturing Engineering*
Universiti Tun Hussein Onn Malaysia, 86400 Parit Raja, Johor, Malaysia

*Corresponding Author: noradila@uthm.edu.my
DOI: https://doi.org/10.30880/rpmme. 026.07.01.013

Article Info

Received: 1 January 2026
Accepted: 1 February 2026
Available online: 28 February 2026

Keywords

VCP, Feldspar, Various types of Clay, Material Characterization, Compression

Abstract

This study use feldspar as a reinforcing material to investigate the compressive strength towards the various types of clay, in this case is SP17B, SP17C, SP22, and SP22B for application of sewage system, Vitrified Clay Pipes (VCP). The raw clay were dried, crushed to powder particle size (micro), sieved to ensure uniform size, compacted into cylinder shape, and sintered with control temperature at 1100ºC with heating and cooling rate around 2 hours with a ramp of 2ºC/min. Clay and feldspar powder is used to determine the material characterization of samples by EDS and TGA test. The results show that all of the materials has highest weight percentage of silicon (Si). Sintered sample will run a compression test, result in sample with 5% of feldspar show a signifciant improvement on compression force and strength, 2.63-5.66kN and 1.98-4.27 Mpa. Hence, the results obtained demonstrates feldspar's potential as an economical and sustainable reinforcement to maximize VCP performance.

1. Introduction

Due to their long lifespan, mechanical durability, and resistance to chemicals, vitrified clay pipes (VCP) are widely used in sewer systems in response to the need for long-lasting and environmentally friendly underground infrastructure. The high-temperature vitrification process used to create VCP produces a dense, non-porous substance that is perfect for wastewater applications. Researchers have investigated using waste-based additives and composite materials in clay pipe production to increase performance while lowering manufacturing costs and environmental impact as environmental sustainability becomes a priority. Pipes made of composite materials can endure harsh conditions while using the fewest resources possible.

In order to improve the material's qualities, a number of researchers have looked into adding industrial waste to clay mixtures. Cement dust was used in clay composites by El Sherbiny et al. (2004), who discovered that it decreased the modulus of rupture (MOR) in unfired samples. By using ceramic sludge, Al Hoseny et al. (2018) saw increases in bulk density and linear firing shrinkage. When glass cullet was added to clay compositions, El-Shimy et al. (2014) found that it decreased porosity and water absorption, improving mechanical strength. These results demonstrate how waste materials can be used to enhance clay composites' mechanical and physical properties. The growing issue of solid waste generation was highlighted by H. Wang et al. (2023), who pointed out that feldspar, which is frequently found in the Earth's crust, contains advantageous fluxing agents (Na_2O) and (K_2O) that are useful in ceramics.

Despite the encouraging results of these investigations, few research has been done clearly to examine how feldspar affects the compressive strength of different types of clay. Feldspar's reaction behaviour varies by type, according to Bozaghian Backman et al. (2024), suggesting that more research is necessary to fully understand how it interacts with various clays. Therefore, the purpose of this study is to evaluate the effect of 5% feldspar reinforcement on the compressive strength of clay Sp17B, SP17C, SP22, and SP22B as well as to characterize the elemental and thermal properties of feldspar. By investigating feldspar's potential to improve the mechanical performance of vitrified clay pipe, this study fills a gap in the literature.

2. Methodology

Methodology refers to the systematic, theoretical analysis of the methods applied to a field of study. It includes the principles, procedures, and practices that guide the conduct of experiments or research. It describes the methodology used in a study so that it can be repeated or assessed by future researchers.

2.1 Preparation of Samples

To begin with, the clay was distributed by JPC Intan Sdn Bhd, a supplier located at Claytan in Ayer Hitam. Firstly, the process started with identifying the types of clay including SP17B, SP17C, SP22, and SP22B. The experimental procedure requires proper preparation using machine provided by Ceramic and Polymer Laboratory.

Table 2.1: Material

Material	Description
	Type of Clay 1. SP17B 2. SP17C 3. SP22 4. SP22B
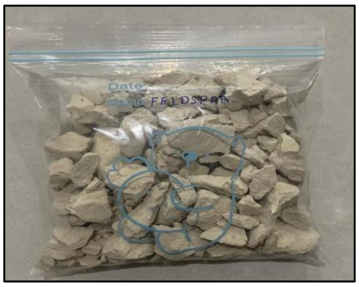	Feldspar

Then, the preparation phase continues with drying the clay samples at 120^{0}C for 24 hours to remove moisture content and ensure consistent starting conditions for next processing steps. After drying phase, the clay undergoes crushing process to create a uniform particle size. Sieving process is the next step to ensure uniform clay powder size, 63µm. This process is crucial for accurate results in further testing and analysis. The sieved clay then proceeds with mixing process with varying composition, where feldspar is added to the raw clay. The specified compositions are 100:0 and 95:5, indicating various types of clay to feldspar that will be tested to determine optimal composition for the intended application.

Table 2.2: Weight Ratio Scale

Type of Clays	Composition of clay and feldspar (%)	
SP17B SP17C SP22 SP22B	(100:0)	(95:5)

The mixing process for powder is part of the mixing stage, where the mixed materials are further processed to achieve fine particle and homogeneous blending. The mixed materials were mill in a cylindrical container with 4 grinding balls and rotated vertically at 100rpm for 30 minutes. After milling, all samples undergo compaction to form test specimens. The cylindrical shapes were formed from a mixture that undergoes mixing phase using compaction technique. The specimens were formed using a mould with specific dimensions which are 13mm in diameter and 26mm in height. The compacted samples is then subjected to a sintering process at 1100^{0}C, which promotes particle bonding and denser of the clay-feldspar mixture. Figure 2.1 shows the sintering profile.

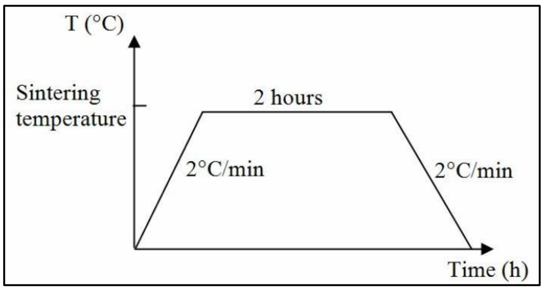

Fig 2.1: Sintering Profile (Jalaluddin et al., 2024)

2.2 Testing

After the mix material composite sintered, several test are conducted to fulfil the research requirement and achieve the objective. The test included Energy Dispersive X-Ray Spectroscopy (EDS), Thermogravimetric Analysis, and Compression Test.

2.2.1 Energy Dispersive X-Ray Spectroscopy (EDS)

The sample in powder particle is put on lab specimen. The specimen is then coated with Gold (Au) to make the specimen conductive. The EDS result obtained together with SEM as the machine is combined. The test is conducted at Material Science Laboratory, UTHM.

2.2.2 Thermogravimetric Analysis (TGA)

Within controlled environment and ambient temperature, the sample specimen is subjected to a controlled temperature program as a function of temperature or time so that the mass of the substance can be measured using Thermogravimetric Analysis. The test is conducted in Ceramic Laboratory, UTHM.

2.2.3 Compression Testing

In mechanics perspective, compressive strength measures the material's ability to withstand crushes under heavy loads. Evaluating structural materials, such as ceramics is crucial as the material must withstand heavy loads and pressure especially in heavy industry, in this case underground structure. The compression test used flat workspace to press the sample to obtain the behaviour under a compressive load. The ASTM used is C1424 Test Method for Monotomic Compressive Strength of Advanced Ceramics at Ambient Temperature, (2019). The crosshead speed rate for comparison is 0.5mm/min.

$$Compressive\ Strength, \sigma = \frac{P}{A} \tag{1}$$

3. Result and Discussion

3.1 Energy Dispersive X-Ray Spectroscopy (EDS)

Figure 3.1 below shows the mineral composition for clay SP17B obtained by EDS test. Based on the EDS graph analyses, the graph indicates that the dominant element in clay is silicon 19.06% and aluminium 10.71%. Although there is minimum presence of sodium, magnesium, and calcium, the role of the element as minor exchangeable cation or structural components Sarani et al., (2023)

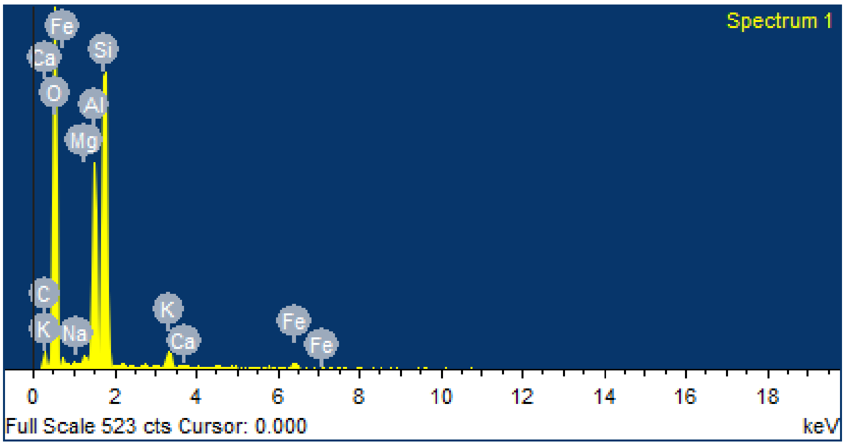

Fig 3.1: EDS analyzed for SP17B

Figure 3.2 below depicted the mineral composition for clay SP17B obtained by EDS test. In keeping with the EDS graph, these indicated that the 2 highest element is silicon (Si) with 24.35% and aluminium (Al) with 14.08% from total weight. This is due to the most clay are aluminosilicates which contain silicon (Si) and aluminium (Al) oxides Hamzawy et al., (2024).

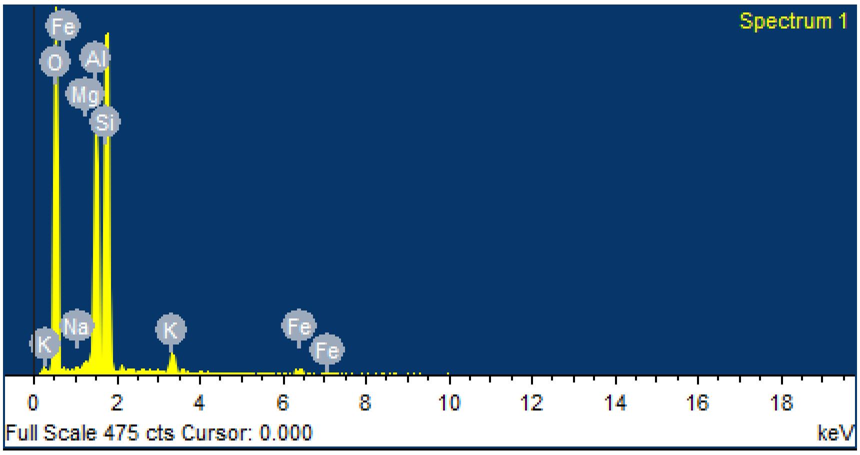

Fig 3.2: EDS analyzed for SP17C

Figure 3.3 illustrates the elemental composition of clay SP22. Throughout the results, SP22 contained the highest element, silicon (Si), accounting for 22.05% from total weight. Moreover, aluminium is the second highest element in clay SP22. This is due to most clays are alluminosilicates, which contain aluminium (Al) and silicon (Si) oxides Hamzawy et al., (2024). Other small amounts of element also recorded which Sarani et al., (2023) addressed the role of these small amounts of minor exchangeable cations or structural components.

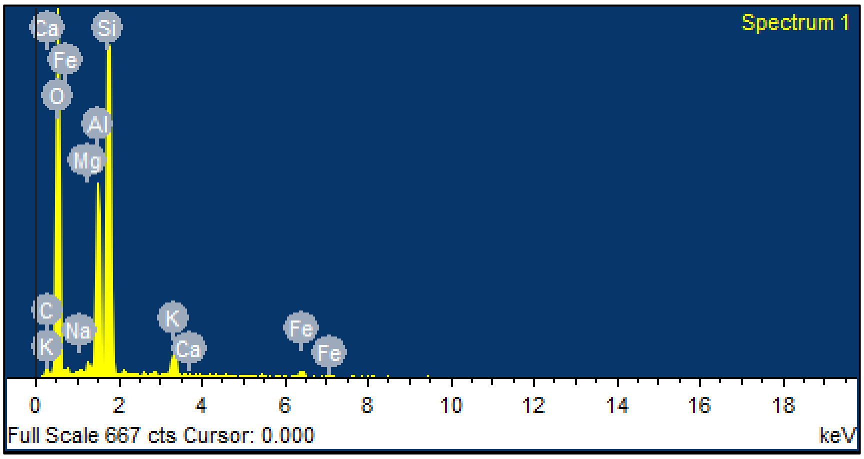

Fig 3.3: EDS analyzed for SP22

Figure 3.4 shows the elemental composition of clay SP22B. Throughout the outcomes, SP22B had the highest concentration of silicon (Si) and aluminium (Al), 23.66% and 11.45% respectively from total weight. Most clays are aluminosilicates, which causing the material to contain highest amounts of silicon (Si) and aluminium (Al) Hamzawy et al., (2024).

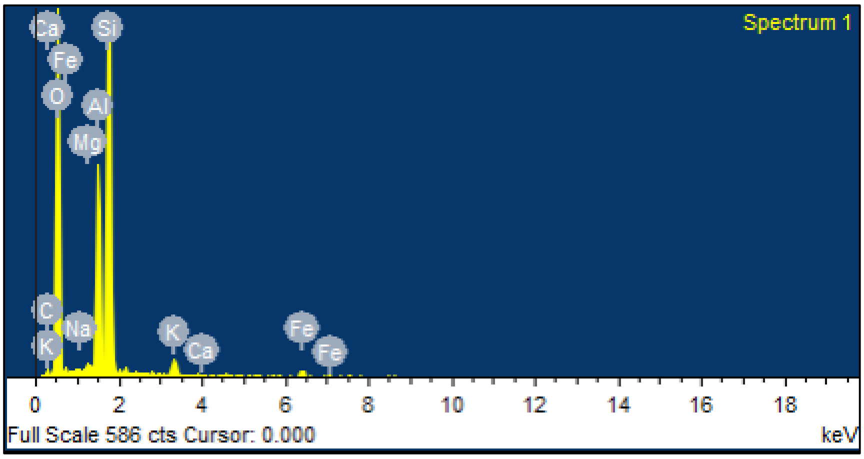

Fig 3.4: EDS analyzed for SP22B

Figure 3.5 shows the results of EDS pattern for feldspar. Based on the EDS graph obtained, it shows high values of silicon (Si) with 28.15% and potassium (K) with 10.2% from total weight showing that this type of feldspar is K-feldspar. Lee et al., (2025) stated that due to the potassium, it results in more homogeneous and denser microstructure. Furthermore, it exhibits fewer pores resulting in enhanced bonding. Egole et al., (2024) confirm that the addition of feldspar can improvise the plastic properties of the materials for manufacturing purpose hence, leading to higher product quality and reduced manufacturing costs. The resulting microstructure validates the mechanical outcomes, which indicate that the physical bonding in microstructure is probably responsible for the increased in compressive strength. Thus, feldspar has been shown to be excellent reinforcement material for clay.

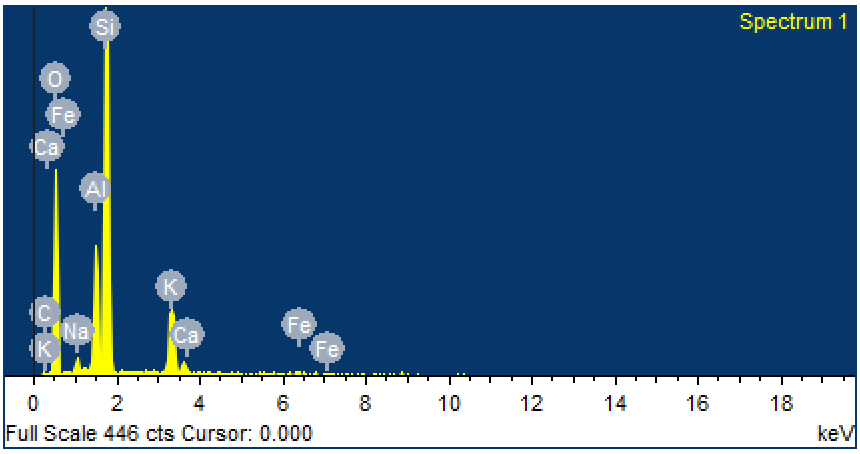

Fig 3.5: EDS analyzed for Feldspar

3.2 Scanning Electron Microscopy

The microstructure of clay ceramic was captured using the Scanning Electron Microscopy (SEM) as shown in figure 3.6 with different magnification ranging from 1000x to 3000x is to verify the fine structure of clay SP17C powder. From the SEM result, the microstructure is compacted and uniform, with firmly compacted particles and tiny pore connectivity. El-Shimy et al., (2024) discovered that usage of clay with additional structures enhanced the bonding in microstructure hence, making the clay become stronger.

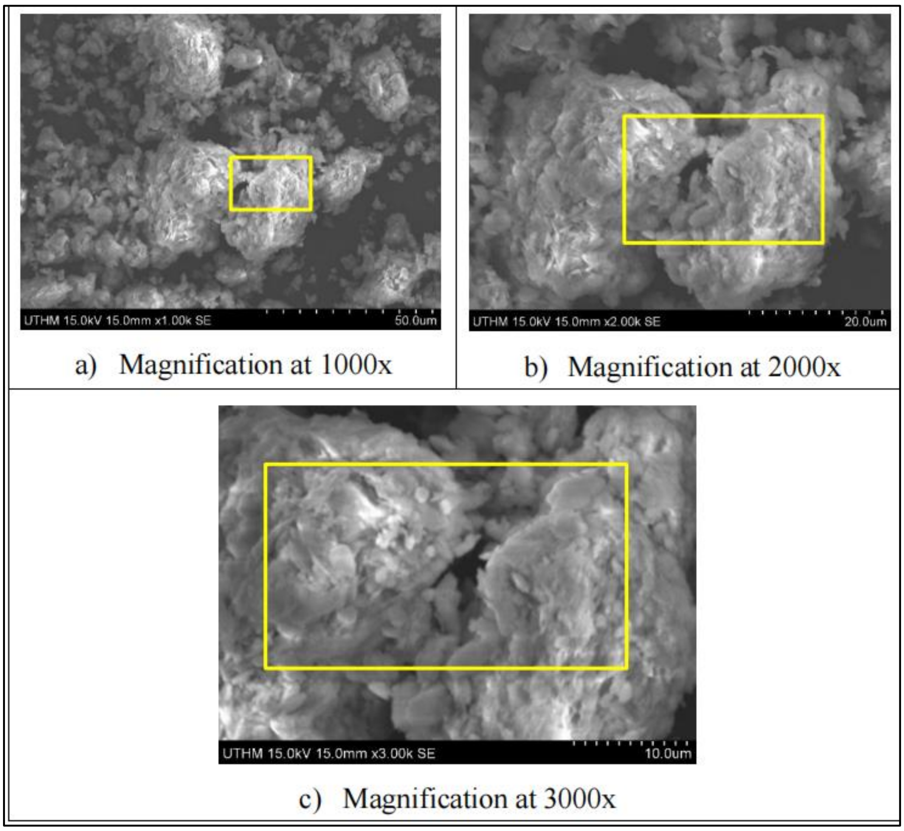

a) Magnification at 1000x
b) Magnification at 2000x
c) Magnification at 3000x

Fig 3.6: SEM for clay SP17B

Based on figure 3.7, Scanning Electron Microscopy (SEM) with different magnification ranging from 1000x to 3000x to verify the fine structure of clay SP17C. At higher level magnification, the image shows more rigidity and dense structure, hence, show improved atomic level bonding between particles. Al Hoseny et al.,(2018) stated that the addition of additional material results in higher mechanical properties than the raw material.

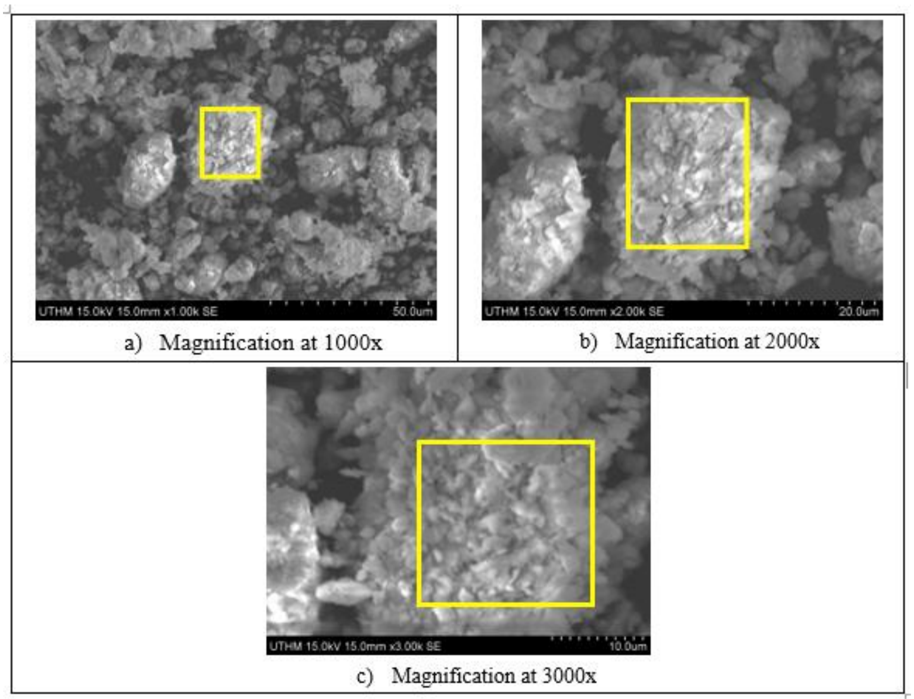

a) Magnification at 1000x
b) Magnification at 2000x
c) Magnification at 3000x

Fig 3.7: SEM for clay SP17C

According to figure 3.8, the microstructure of clay SP22 is compact and uniform, with tightly packed particles and tiny pore on 3000x magnification. As a result, it demonstrates improved atomic level bonding between particles. El-Shimy et al., (2014) utilizing clay with additional structures improved bonding resulting in a stronger clay.

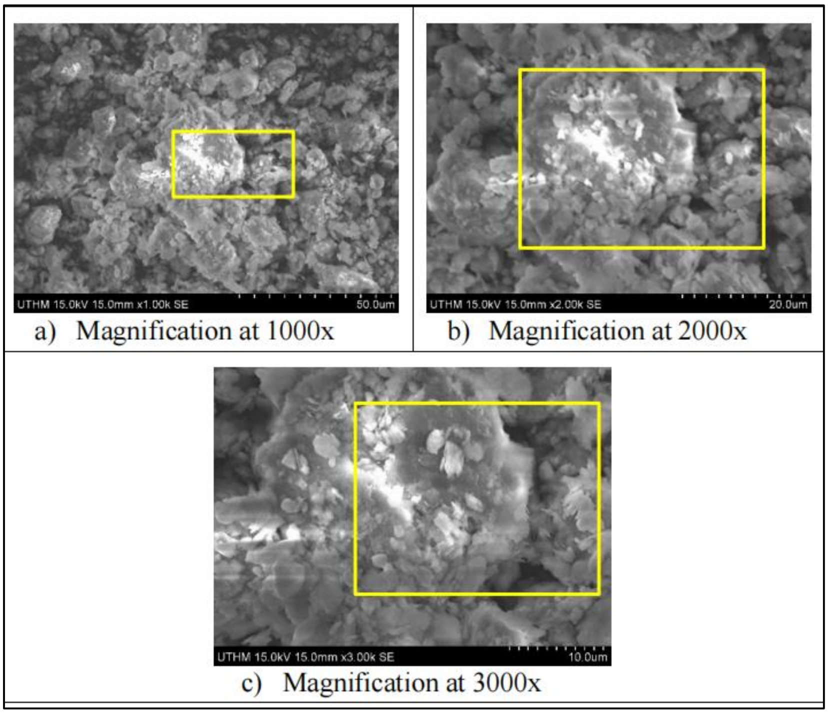

Fig 3.8: SEM for clay SP22

As indicated in figure 3.9, the microstructure is dense and uniform at 3000x magnification implying that the material is stronger. Al Hoseny et al., (2018) stated that adding more material results in higher mechanical properties than using simply the raw material, in this case clay.

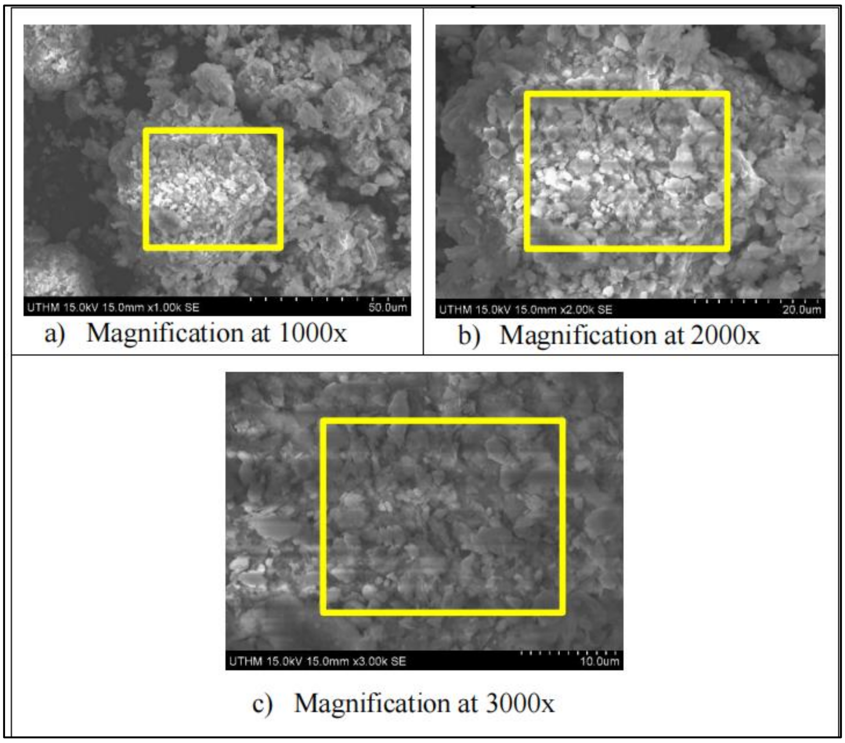

Fig 3.9: SEM for clay SP22B

Figure 3.10 illustrates the Scanning Electron Microscopy (SEM) analysis of feldspar shows different level of magnification from 1000x to 3000x. Lee et al., (2025) stated that the feldspar is more homogeneous, denser, and exhibits fewer pores resulting in enhanced bonding. Egole et al., (2024) found that by adding feldspar as reinforcement material improvise the plastic properties of the material composition. Thus, feldspar has been shown to be an excellent reinforcement material for clay.

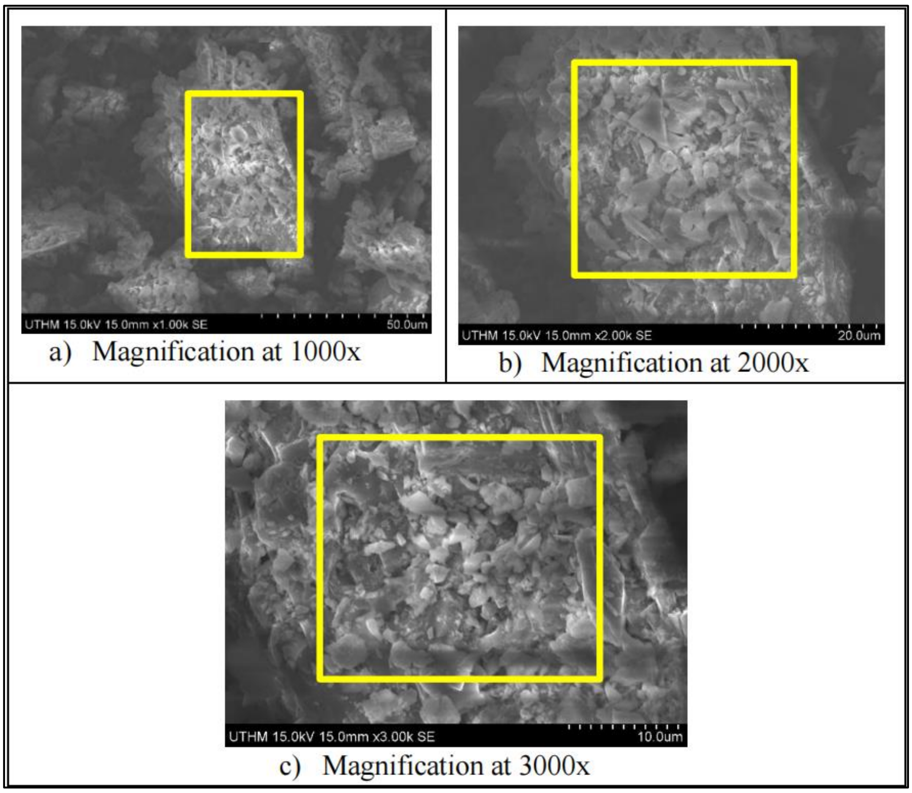

Fig 3.10: SEM for feldspar

3.3 Thermogravimetric Analysis (TGA)

Element decomposition of clay was determined by using Thermogravimetric Analysis (TGA) as shown in figure 3.11. The results for clay SP17B reveal a total mass loss with obvious decomposition at temperatures from 150ºC to 700ºC. The evaporation of physically adsorbed moisture is responsible for the initial, significant weight loss up to about 150ºC. A slow mass decrease between 150ºC to 500ºC indicates the dihydroxylation of clay minerals such as kaolinite or illite, which results in the release of structural water El-Desoky et al., (2019). The sample demonstrates thermal stability above 700ºC with negligible changes up to 1300ºC, implying the completion of significant decomposition processes. Wang et al., (2021) stated that the mass loss due to high concentration of volatile and decomposable materials.

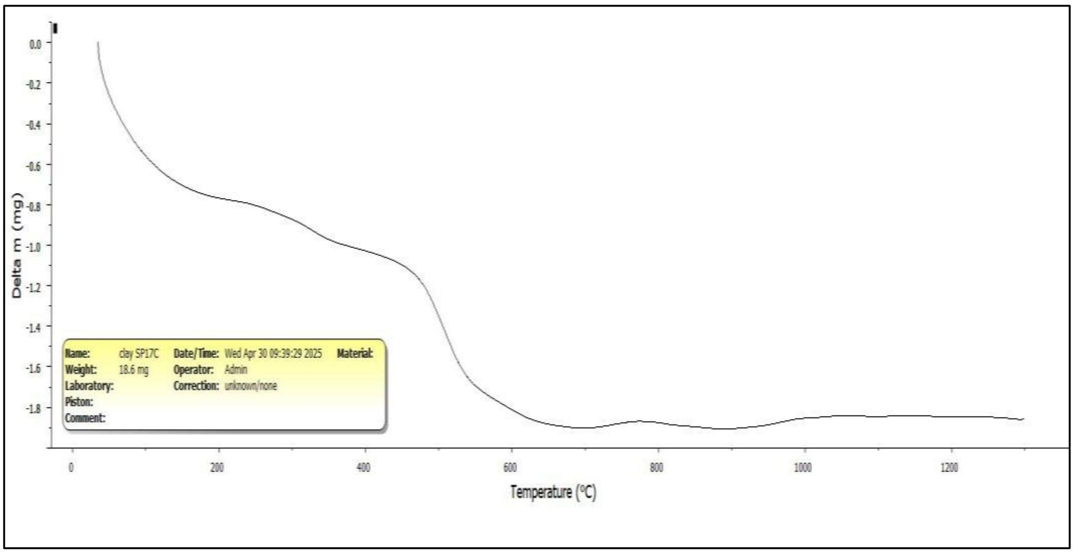

Fig 3.11: TGA data on clay SP17B

Based on figure 3.12, the TGA illustrates the temperature range covered by the assessment is 0^0C to roughly 1100^0C. The sample begins to lose weight up to about 300^0C, which suggest that moisture or volatiles are probably being removed as the material moves from ambient to moderate temperatures. Phonphuak et al., (2019) The rate of weight loss increases as the temperature rises above 300^0C but reaches a significant tipping point at 600^0C, where an obvious and fast weight loss is seen. This might signal the beginning of the material's thermal breakdown. Alabduljabbar et al., (2021) stated that this is due to structural disintegration and the release of volatiles and may reflect phase transitions or modifications in the material's chemical structure.

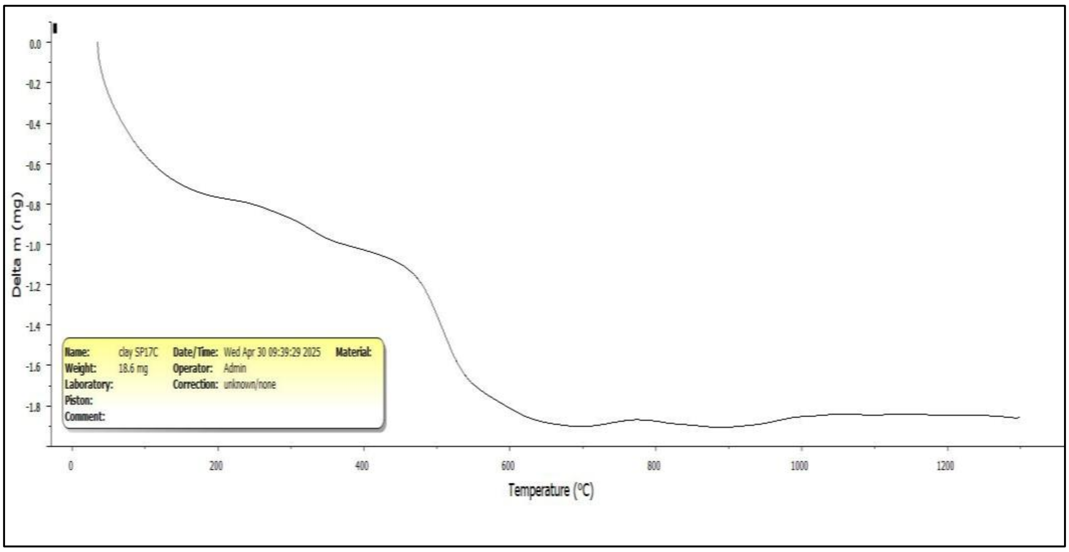

Fig 3.12: TGA data on clay SP17C

Figure 3.13 illustrates the TGA data for clay SP22 showed the decomposition of the sample's reflected in a more significant mass due to mass decrease as the temperature rises above this first point. The substantial weight loss seen in the temperature range of roughly 300^0C to 600^0C points to the breakdown of the primary structural elements, which releases volatile degradation products due to burning process Xie et al., (2024). The existence of thermally stable inorganic remains that do not decompose within the temperature range under study indicated by the residual mass at higher temperatures. The information suggests that the material degrades in stages, starting with moisture loss, then organic component degradation, and ending with the formation of a stable residue. These revelations are essential for comprehending the material's thermal behaviour and possible application boundaries at high temperatures. El-Desoky et al., (2019)

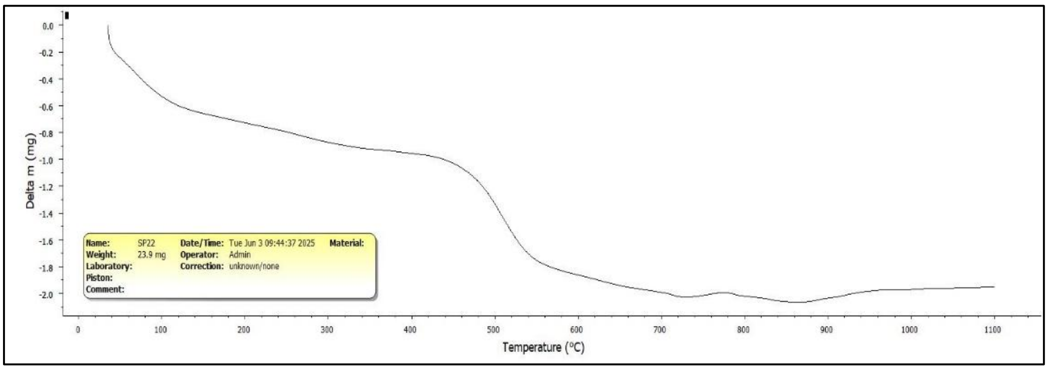

Fig 3.13: TGA data on clay SP22

Based on figure 3.14, the sample exhibits a slow mass loss up to roughly 300^{0}C, which is probably caused by the removal of low-temperature volatile compounds and the evaporation of physically adsorbed water Wang et al., (2021). This phase's mass loss seems to be gradual and minimal, suggesting that thermal behaviour in this temperature range is comparatively stable. The thermal decomposition of organic matter or other thermally unstable components in the sample is suggested by known mass loss that can be observed between 300^{0}C to 600^{0}C. This drop suggests the existence of important components that oxidize or decomposed in this range. The curve stabilizes at 600^{0}C then shows a slight upward trend beyond 800^{0}C, which Sarani et al., (2023) explained that it could be due to oxidative reactions or the creation of new phases, such as metal oxide formation, that gain mass through oxidation.

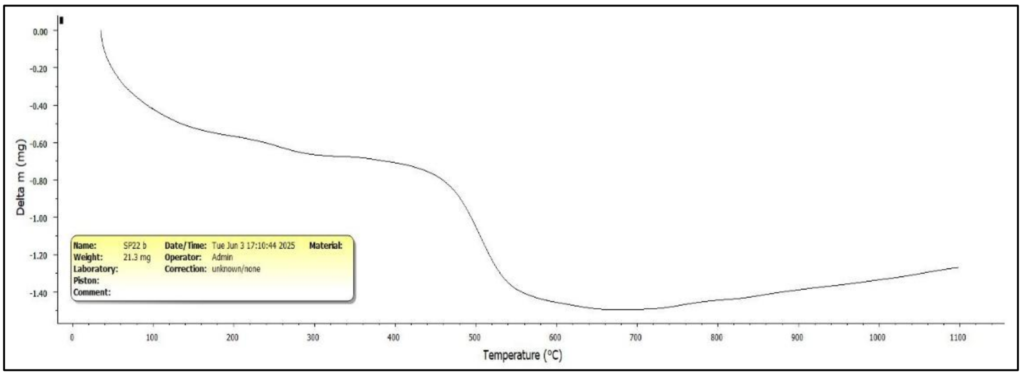

Fig 3.14: TGA data on clay SP22B

Figure 3.15 depicted the data of TGA for feldspar. During the first stage, the mass decreases steadily up to around 200^{0}C. This region likely represents the loss of physically adsorbed water or surfaced-bound moisture. Feldspar minerals can adsorb small amount of moisture, which is usually released at low temperatures Krzywinski et al., (2023). Throughout the second stage which around 200^{0}C to 600^{0}C, the possible dihydroxylation or loss of structural hydroxyl groups result in minor fluctuations and continued weight loss Hamzawy et al., (2024). A notable mass gain begins around 750^{0}C to 900^{0}C then, a sharp mass increase from 950^{0}C to 1300^{0}C. This could be due to high-temperature sintering reactions, phase transformations, or oxygen incorporation.

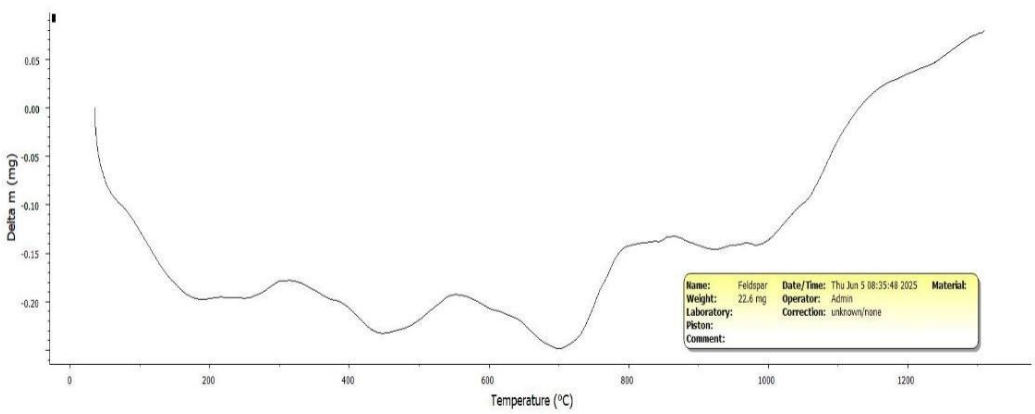

Fig 3.15: TGA data on feldspar

3.4 Compression Strength of Clay Composites

Table 3.1 lists the results of compression force and strength obtained from Solid Mechanic Laboratory, FKMP, UTHM. Figure 3.16 and 3.17 shows the trend of compression strength at different types of clay with 2 different compositions.

Table 3.1: Compression Force and Compression Strength of Clay composites

Sample	Ratio (%)	Compression Force, kN	Compression Strength (MPa)
SP17B	100:0	2.50	1.88
	95:5	2.63	1.98
SP17C	100:0	2.32	1.75
	95:5	3.18	2.40
SP22	100:0	3.95	2.98
	95:5	3.89	2.93
SP22B	100:0	3.34	2.80
	95:5	5.66	4.27

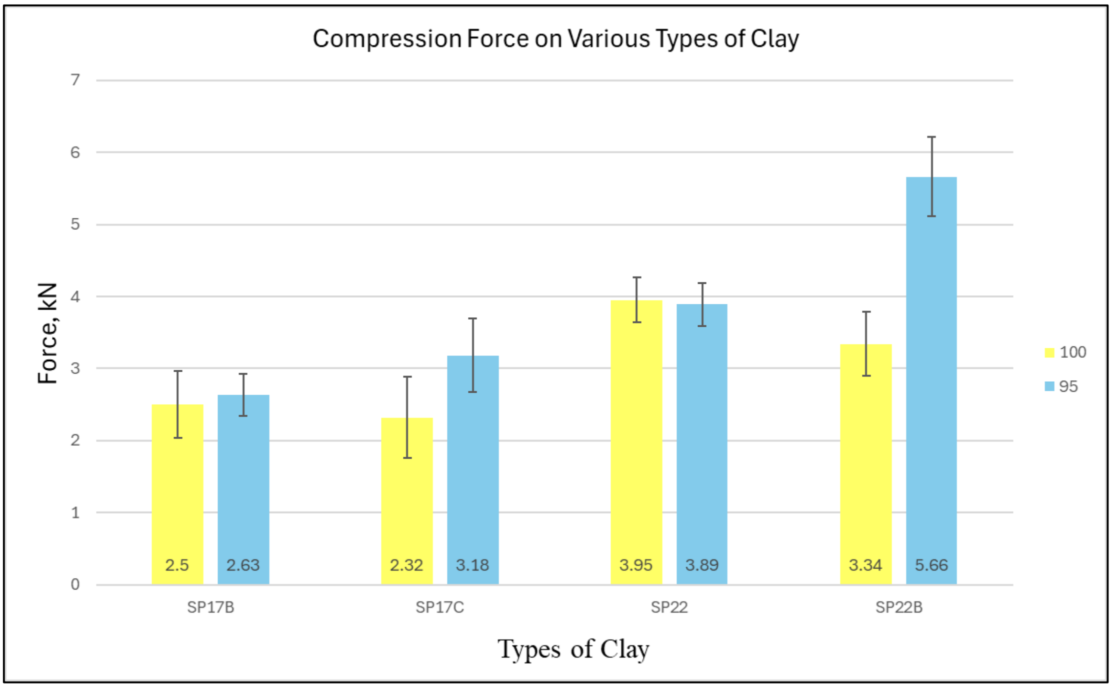

Figure 3.16: Compression force for several types of clay composite

In keeping with Figure 3.16 and Figure 3.17, compression results show by addition of feldspar as a reinforcement agent towards several types of clay significantly increases its mechanical force and strength. Overall, comparison for 100% clay mix, the compressive force for all types of clay in 95% clay mix shows a greater value. In the meantime, the compressive strength for 95% clay mix shows a higher value on clay SP22B with 5.66kN. The range for 100% clay mix shows a range of 2.5kN to 3.34kN. Meanwhile, the 95% clay mix range from 2.63kN to 5.66kN. This can be concluded that by addition of feldspar, can enhanced the bonding and denser microstructure. As defined by Krzywinski et al., (2023), enhanced bonding helps to distribute stress more effectively and improves overall strength of one material. In comparison to previous researchers using cullet El-shimy et al., (2014), feldspar provides better strength.

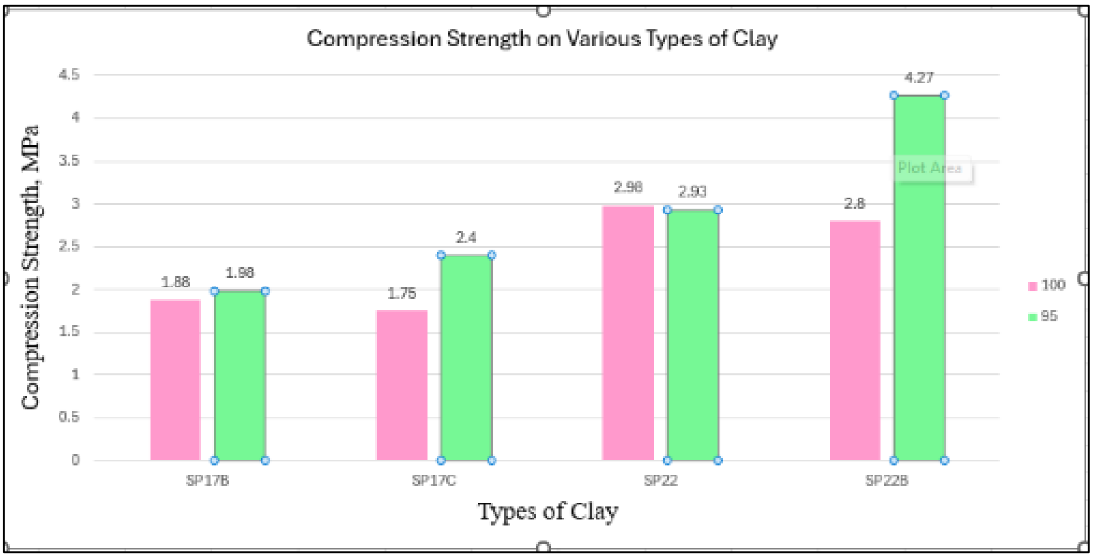

Figure 3.17: Compression Strength for several types of clay composite

Based on tabulated chart on figure 3.17, the data obtained averagely can conclude that clay (95%) with mixture of feldspar (5%) shows a greater value than raw clay (100%). This resulting in agreement with Krzywinski et al., (2023) which state that a mixture of more than one material can enhanced the mechanical properties of composite materials. Feldspar, as reinforcement material act as fluxing agent resulting in more homogeneous, denser, and exhibits fewer pores. This resulting in enhanced mechanical properties and strength in material composite inner structure.

Lastly, the compression curve rapidly decreases after reaching peak load meaning brittle failure, which is typical of ceramic-like materials such as clay and concrete. The material's low plastic deformation capability causes this brittle behaviour once microcracks form since they happen quickly with little warning.

4. Conclusion

In conclusion, based on the EDS results obtained, the elemental composition of various types of clay exhibits the highest value of silicon (Si) and aluminium (Al) while feldspar contain the highest value of potassium (K) and silicon (Si). The highest value of silicon act as basic building blocks of clay minerals while feldspar act as fluxing agent contained homogeneous, denser, and exhibit fewer pores resulting in enhanced bonding. The compression strength can be conclude that by adding only 5% of feldspar can increase the compression strength compare to 0% of feldspar. This is due to the feldspar microstructure which is denser and acts as fluxing agent resulting in increase the strength of clay.

Acknowledgement

The authors would like to acknowledge the Faculty of Mechanical and Manufacturing Engineering in Universiti Tun Hussein Onn Malaysia for the support and acknowledged to the company JPC-Intan sdn Bhd that supplied the research material.

References

[1] Krzywiński, K., Sadowski, Ł., Fedoruk, K., & Sieradzki, A. (2022). Fundamental understanding of the thermal properties of amorphous epoxy resin coatings filled with quartz-feldspar powder sourced from quarry waste. *Applied Surface Science*, *614*, 156133. https://doi.org/10.1016/j.apsusc.2022.156133

[2] Sarani, N. A., Kadir, A. A., Din, M. F. M., Hashim, A. A., Hassan, M. I. H., Hamid, N. J. A., Hashar, N. N. H., Hissham, N. F. N., & Johan, S. F. S. (2023). Physical-mechanical properties and thermogravimetric analysis of fired clay brick incorporating palm kernel shell for alternative raw materials. *Construction and Building Materials*, *376*, 131032. https://doi.org/10.1016/j.conbuildmat.2023.131032

[3] Phonphuak, N., Saengthong, C., & Srisuwan, A. (2019). Physical and mechanical properties of fired clay bricks with rice husk waste addition as construction materials. *Materials Today: Proceedings*, *17*, 1668–1674. https://doi.org/10.1016/j.matpr.2019.06.197

[4] El-Shimy, Y. N., Amin, S. K., El-Sherbiny, S. A., & Abadir, M. F. (2014). The use of cullet in the manufacture of vitrified clay pipes. *Construction and Building Materials*, *73*, 452–457. https://doi.org/10.1016/j.conbuildmat.2014.09.090

[5] El-Desoky, H., Farouk, S., Heikal, M., El-Mahallawy, M., & Wahid, A. (2019). Geochemical and technical investigation of some clay materials in the Bahariya Oasis, Western Desert, Egypt: Implication in the vitrified clay pipes industry. *Journal of African Earth Sciences*, *160*, 103612. https://doi.org/10.1016/j.jafrearsci.2019.103612

[6] Egole, C. P., Medupin, R. O., Nzebuka, G. C., Nnodum, N. A., Ochieze, U. P., Eterigho-Ikelegbe, O., Wilson, U. N., & Yoro, K. O. (2024). Quartz and feldspar- blended clay composites for thermal and structural applications. *Results in Materials*, *23*, 100584. https://doi.org/10.1016/j.rinma.2024.100584

[7] El Sherbiny, S. A., Youssef, N. F., Ibrahim, O. A., & Abadir, M. F. (2004). Use of cement dust in the manufacture of vitrified sewer pipes. *Waste Management*, *24*(6), 597–602. https://doi.org/10.1016/j.wasman.2004.01.007

[8] Bozaghian Bäckman, M., Rebbling, A., Kuba, M., Larsson, S. H., & Skoglund, N. (2024). Bed material performance of quartz, natural K-feldspar, and olivine in bubbling fluidized bed combustion of barley straw. *Fuel*, *364*, 130788. https://doi.org/10.1016/j.fuel.2023.130788

[9] Alabduljabbar, H., Benjeddou, O., Soussi, C., Khadimallah, M. A., & Alyousef, R. (2021). Effects of incorporating wood sawdust on the firing program and the physical and mechanical properties of fired clay bricks. *Journal of Building Engineering*, *35*, 102106. https://doi.org/10.1016/j.jobe.2020.102106

[10] Al Hoseny, N. F., Amin, S. K., Fouad, M. M. K., & Abadir, M. F. (2018). Reuse of ceramic sludge in the production of vitrified clay pipes. *Ceramics International*, *44*(11), 12420–12425. https://doi.org/10.1016/j.ceramint.2018.04.031

[11] Lee, Y., Shih, H., & Widyastuti, E. (2025). A novel development of renewable feldspar from oyster shells powder and fly ash. *Ceramics International*. https://doi.org/10.1016/j.ceramint.2025.03.002

[12] Huang, W., Yang, Y., Gui, W., Liu, J., Lv, Y., Wang, Z., & Xia, Q. (2023). Nitrogen impacts on structural stability of feldspar: Constraints from high temperature and high pressure spectroscopy and machine learning. *Physics of the Earth and Planetary Interiors*, *336*, 106997. https://doi.org/10.1016/j.pepi.2023.106997